Synthesis, Light Emission, Nanoaggregation, and Restricted Intramolecular Rotation of 1,1-Substituted 2,3,4,5-Tetraphenylsiloles

Junwu Chen,† Charles C. W. Law,† Jacky W. Y. Lam,† Yuping Dong,† Samuel M. F. Lo,† Ian D. Williams,† Daoben Zhu,‡ and Ben Zhong Tang*,†

Department of Chemistry, Center for Display Research, Institute of Nano Science and Technology, and Open Laboratory of Chirotechnology of the Institute of Molecular Technology for Drug Discovery and Synthesis, Hong Kong University of Science and Technology, Clear Water Bay, Kowloon, Hong Kong, China, and Center for Molecular Science, Institute of Chemistry, Chinese Academy of Sciences, Beijing 100080, China

Received November 14, 2002. Revised Manuscript Received January 29, 2003

A series of ten 2,3,4,5-tetraphenylsiloles with different 1,1-substituents [XYSi(CPh)$_4$] were prepared, and three of these, i.e., 1,1,2,3,4,5-hexaphenylsilole [X = Y = Ph (**3**)], 1-ethynyl-1,2,3,4,5-pentaphenylsilole [X = Ph, Y = C≡CH (**15**)], and 1,1-bis(phenylethynyl)-2,3,4,5-tetraphenylsilole [X = Y = C≡CPh (**18**)], were characterized crystallographically. The ground- and excited-states of the siloles were influenced by the inductive effect of the 1,1-substituents: with an increase in their electronegativity, the absorption and emission spectra of the siloles bathochromically shifted. A simple and reliable TLC-based method was developed for measurement of the solid-state luminescence spectra of the siloles. When molecularly dissolved in common solvents at room temperature, all the siloles were practically nonemissive ("off"). When poor solvents were added, the silole molecules clustered into nanoaggregates, which turned the emission "on" and boosted the photoluminescence quantum yields by up to 2 orders of magnitude (aggregation-induced emission). The silole emission could also be greatly enhanced by increasing the viscosity and decreasing the temperature of the silole solutions. The solution thickening and cooling experiments suggest that the aggregation-induced emission is caused by the restricted intramolecular rotations of the peripheral aromatic rings upon the axes of the single bonds linked to the central silole cores.

Introduction

Siloles or silacyclopentadienes are a group of five-membered silacycles that possess unique low-lying LUMO level associated with the $\sigma^*-\pi^*$ conjugation arising from the interaction between the σ^* orbital of two exocyclic σ-bonds on the silicon atom and the π^* orbital of the butadiene moiety.[1] Siloles exhibit high electron acceptability[1,2] and fast electron mobility[3] and have been utilized as electron-transporting and light-emitting layers in the fabrication of electroluminescence (EL) devices.[3,4] We have recently observed an intriguing *aggregation-induced emission* (AIE) phenomenon in a silole system:[5] 1-methyl-1,2,3,4,5-pentaphenylsilole[6] (**2**; Chart 1) is virtually nonemissive in ethanol solutions (Φ_F = 0.06%) but its aggregates or films are highly luminescent (Φ_F = 21%). A light-emitting diode (LED) of **2** exhibited excellent EL performance, with maximum current (CE) and power efficiencies (PE) of 20 cd/A and 14 lm/W, respectively. The maximum external quantum efficiency (η_{EL}) of the EL device was 8%,[5,7] approaching the limit of the possible.[8,9] Clearly, silole **2** is an

* To whom correspondence should be addressed at the Department of Chemistry, Hong Kong University of Science and Tecchnology. Phone: +852-2358-7375; Fax: +852-2358-1594; E-mail: tangbenz@ust.hk. Additional affiliations for this author include the following: Center for Display Research and Institute of Nano Science and Technology, Hong Kong University of Science and Technology, and Open Laboratory of Chirotechnology of the Institute of Molecular Technology for Drug Discovery and Synthesis (supported by an Area of Excellence (AoE) Scheme administered by the University Grants Committee of Hong Kong).

† Department of Chemistry, Hong Kong University of Science and Technology.

‡ Center for Molecular Science, Chinese Academy of Sciences.

(1) For reviews, see the following. (a) Sadimenko, A. P. *Adv. Heterocycl. Chem.* **2001**, *79*, 115−197. (b) Lee, V. Y.; Sekiguchi, A.; Ichinohe, M.; Fukaya, N. *J. Organomet. Chem.* **2000**, *611*, 228−235. (c) Yamaguchi, S.; Tamao, K. *J. Chem. Soc., Dalton Trans.* **1998**, 3693−3702. (d) Wrackmeyer, B. *Coord. Chem. Rev.* **1995**, *145*, 125−156. (e) Chuit, C.; Corriu, R. J. P.; Reye, C.; Young, J. C. *Chem. Rev.* **1993**, *93*, 1371−1448.

(2) Among conjugated five-membered heterocyclics (pyrrole, thiophene, furan, etc.), siloles have the highest electron-accepting ability.[1]

(3) An electron mobility as high as 2 × 10^{-4} cm^2/(V s) was reported for a silole molecule, 2,5-bis(2, 2′-bipyridin-6-yl)-1,1-dimethyl-3,4-diphenylsilole, at an electrical strength of 640 kV/cm. Murata, H.; Malliaras, G. G.; Uchida, M.; Shen, Y.; Kafafi, Z. H. *Chem. Phys. Lett.* **2001**, *339*, 161−166.

(4) (a) Murata; H.; Kafafi; Z. H.; Uchida; M. *Appl. Phys. Lett.* **2002**, *80*, 189−191. (b) Ohshita, J.; Kai, H.; Takata, A.; Iida, T.; Kunai, A.; Ohta, N.; Komaguchi, K.; Shiotani, M.; Adachi, A.; Sakamaki, K.; Okita, K. *Organometallics* **2001**, *20*, 4800−4805. (c) Hay, C.; Hissler, M.; Fischmeister, C.; Rault-Berthelot, J.; Toupet, L.; Nyulaszi, L.; Reau, R. *Chem. Eur. J.* **2001**, *7*, 4222−4236. (d) Yamaguchi, S.; Endo, T.; Uchida, M.; Izumizawa, T.; Furukawa, K.; Tamao, K. *Chem. Eur. J.* **2000**, *6*, 1683−1692.

(5) (a) Luo, J.; Xie, Z.; Lam, J. W. Y.; Cheng, L.; Chen, H.; Qiu, C.; Kwok, H. S.; Zhan, X.; Liu, Y.; Zhu, D.; Tang, B. Z. *Chem. Commun.* **2001**, 1740−1741. (b) Freemantle, M. *Chem. Eng. News* **2001**, *79* (41), 29.

(6) Tang, B. Z.; Zhan, X.; Yu, G.; Lee, P. P. S.; Liu, Y.; Zhu, D. *J. Mater. Chem.* **2001**, *11*, 2874−2978.

10.1021/cm021715z CCC: $25.00
Published on Web 03/08/2003

Chart 1

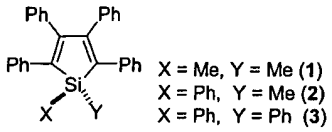

outstanding light-emitting material with unusual luminescence characteristics.

Aggregation of organic molecules often quenches light emission, which has been a thorny problem in the development of efficient LED systems because the organics are normally used as thin solid films in the EL devices.[5,10] In this regard, the AIE feature of **2** is an invaluable property because aggregation is inherently accompanying the film formation.[11] To know whether the AIE is an isolated phenomenon associated with **2** only or a general characteristic for all silole molecules, in this work, we synthesized a series of ten silole derivatives (**1**–**3** in Chart 1 and **13**–**19** in Schemes 1 and 2) and studied their optical properties. We systematically varied the 1,1-substituents of the siloles, in the hope of learning how the molecular structures affect their luminescence properties. In our previous work, we speculated that the molecules of silole **2** might have aggregated into nanoclusters in its poor solvents;[5] in this work, we experimentally proved our early hypothesis: the silole molecules did form nanoaggregates of different sizes upon addition of large amounts of poor solvents into their solutions. To gain mechanistic insights, we investigated the effects of solvent polarity and solution viscosity as well as temperature on the photoluminescence (PL) behaviors of the siloles. The results suggest that *restricted intramolecular rotation* is the cause for the AIE phenomenon.

Results and Discussion

Silole Synthesis. A series of ten 1,1-substituted 2,3,4,5-tetraphenylsiloles, some of which are new compounds, were prepared via different synthetic routes.

Scheme 1

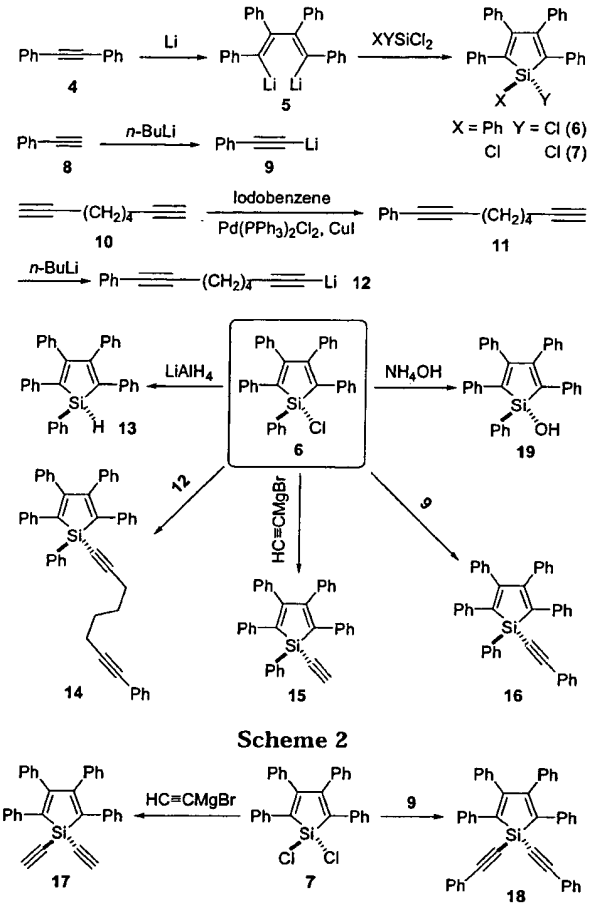

Scheme 2

Siloles **1**, **2**, and **3** were synthesized according to published procedures[6] by the ring-closing reactions of 1,4-dilithio-2,3,4,5-tetraphenyl-1,3-butadiene (**5**) with dichlorodimethylsilane, dichloromethylphenylsilane, and dichlorodiphenylsilane, respectively. The reactions of **5** with trichlorophenylsilane and silicon(IV) chloride afforded, respectively, 1-chloro-1,2,3,4,5-pentaphenylsilole (**6**) and 1,1-dichloro-2,3,4,5-tetraphenylsilole (**7**), from which siloles **13**–**19** were prepared (Schemes 1 and 2).

Chlorosiloles **6** and **7** are important intermediates for silole derivatizations; however, their preparations have been difficult. Curtis prepared the two chlorosiloles by first reacting tolan **4** with an excessive amount of lithium metal and then treating the resultant 1,4-dilithio-2,3,4,5-tetraphenyl-1,3-butadiene (**5**) with trichlorophenylsilane and silicon(IV) chloride.[12] This synthetic route suffers, however, from several drawbacks. The use of excess amount of lithium in the preparation of **5** can easily cause side reactions, leading to the formation of byproducts such as triphenylnaphthalene, as evidenced by the color change of the reaction mixture from dark green to brownish-violet when the reaction time is prolonged.[13] To avoid the side reactions, a short reaction time is necessary (<2 h as advised by Curtis[12]); doing so, however, results in a low conversion of tolan to **5**. The existence of the unreacted lithium metal in the reaction mixture can cause further complications when

(7) (a) Chen, H. Y.; Lam, J. W. Y.; Luo, J. D.; Ho, Y. L.; Tang, B. Z.; Zhu, D. B.; Wong, M.; Kwok, H. S. *Appl. Phys. Lett.* **2002**, *81*, 574–576. (b) Chen, J.; Xie, Z. Lam, J. W. Y.; Kwok, H. S.; Tang, B. Z. *Macromolecules* **2003**, *36*, 1108–1117.

(8) The highest external quantum efficiency for a singlet emitter has been theoretically predicted to be ~5.5%, but recent research in the area suggests that this limit may be lifted to ~8–9%.[9]

(9) (a) Cao, Y.; Parker, I. D.; Yu, G.; Zhang, C.; Heeger, A. J. *Nature* **1999**, *397*, 414–417. (b) Kim, J. S.; Ho, P. K.; Greenham, N. C.; Friend, R. H. *J. Appl. Phys.* **2000**, *88*, 1073–1081. (c) Wohlgenannt, M.; Tandon, K.; Mazumdar, S.; Ramaesha, S.; Vardeny, Z. V. *Nature* **2001**, *409*, 494–497.

(10) (a) Cacialli, F.; Wilson, J. S.; Michels, J. J.; Daniel, C.; Silva, C.; Friend, R. H.; Severin, N.; Samorì, P.; Rabe, J. P.; O'Connell, M. J.; Taylor, P. N.; Anderson, H. L. *Nat. Mater.* **2002**, *1*, 160–164. (b) Tang, B. Z.; Saravanamuttu, K. *Heart Cut* Dec. 2, 2002; http://chemistry.org/heartcut.html. (c) An, B.-K.; Kwon, S.-K.; Jung, S.-D.; Park, S. Y. *J. Am. Chem. Soc.* **2002**, *124*, 14410–14415. (d) Tang, B. Z. *Heart Cut* Dec. 9, 2002; http://chemistry.org/heartcut.html. (e) Sarker, A. M.; Ding, L. M.; Lahti, P. M.; Karasz, F. E. *Macromolecules* **2002**, *35*, 223–230. (f) Chen, S. H.; Su, A. C.; Huang, Y. F.; Su, C. H.; Peng, G. Y.; Chen, S. A. *Macromolecules* **2002**, *35*, 4229–4232. (g) Liu, J.; Shi, Y. J.; Yang, Y. *Appl. Phys. Lett.* **2001**, *79*, 578–580. (h) Deans, R.; Kim, J.; Machacek, M. R.; Swager, T. M. *J. Am. Chem. Soc.* **2000**, *122*, 8565–8566. (i) Nguyen, T. Q.; Kwong, R. C.; Thompson, M. E.; Schwartz, B. J. *Appl. Phys. Lett.* **2000**, *76*, 2454–2456. (j) Zhang, X. J.; Shetty, A. S.; Jenekhe, S. A. *Macromolecules* **1999**, *32*, 7422–7429.

(11) *Film Formation in Coatings: Mechanisms, Properties, and Morphology*; Provder, T., Urban, M. W., Eds.; American Chemical Society: Washington, DC, 2001.

(12) Curtis, M. D. *J. Am. Chem. Soc.* **1969**, *91*, 6011–6018.

the mixture is added into a chlorosilane solution. Gilman et al. thus recommended that the use of an excess amount of lithium in the preparation of siloles should be carefully avoided.[14]

We initially followed the Curtis' procedures[12] but encountered great difficulty in obtaining our desired silole products. We thus modified the reaction procedure and used an excess amount of tolan, instead of lithium, in the preparation of the intermediate **5**. This allowed the lithiation reaction to be carried out for an extended period of time to afford **5** in a high yield (~90%, as estimated by a quenching reaction of **5** by water[6]). The green reaction mixture did not change color in as long as 18 h, so the solution of **5** could be added in a dropwise fashion to the trichlorophenylsilane or silicon(IV) chloride solution. After the addition, the mixture was allowed to reflux for 3−5 h and the reaction proceeded steadily to yield a dark yellow solution of chlorosilole **6** or **7**.

Upon cooling to room temperature, **6** was transformed to siloles **13**−**16** and **19** by the reactions given in Scheme 1[12] and **7** was converted to siloles **17** and **18** following the paths depicted in Scheme 2.[15] The unreacted tolan was easily separated from the silole products by column chromatography[16] and could be recycled and reused. Siloles **13**−**19** were prepared in 30−60% yields, based on the amounts of trichlorophenylsilane and silicon(IV) chloride used, which were far better than what we could achieve with the Curtis' procedures. All the silole products were characterized by spectroscopic methods, from which satisfactory analysis data corresponding to their expected molecular structures were obtained (see Experimental Section for details).

Crystal Structures. Single crystals of three silole compounds, i.e., **3**, **15**, and **18**, were grown from methanol or toluene/heptane mixtures as large fluorescent yellow-greenish blocks. Suitable specimens for data collection were mounted in air on glass fibers and their X-ray diffraction intensity data were collected on a diffractometer. The ORTEP drawings of the siloles are shown in Figure 1 and their crystal data and analysis parameters are summarized in Table 1. Silole **3** crystallized in the triclinic system space group $P\bar{1}$, while siloles **15** and **18** crystallized in the monoclinic system space group $P2_1/c$. Although some difficulty was encountered with **3**, which appeared to suffer from crystal twinning, the structure refinements proceeded generally to acceptable models, with reasonable discrepancy indices, esds, and residual electron densities. The geometric parameters from all the three siloles are in excellent general agreement and selected bond lengths and angles are listed in Table 2.

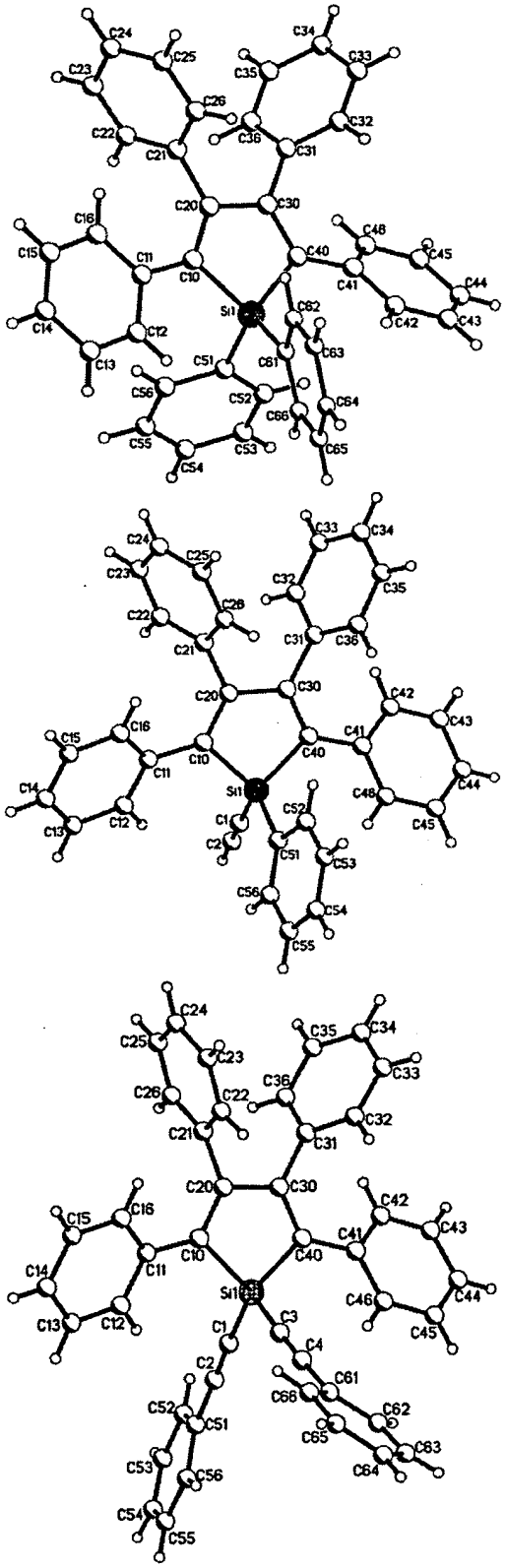

Figure 1. ORTEP drawings of **3**, **15**, and **18** (top to bottom) with atom-labeling schemes for Table 2.

Search of the Cambridge Structural Database (CSD version 5.23) revealed that this class of molecules has been structurally characterized in some depth previously. For silacyclopentadienes, 51 hits were found, and

(13) (a) Braye, E. H.; Hubel, W.; Caplier, I. *J. Am. Chem. Soc.* **1961**, *83*, 4406−4413. (b) This point has been reemphasized by Ferman et al. in a recent publication on the syntheses of **1** and **3**, in which the authors advised that the mixtures should not be stirred for too long because "longer reaction times can lead to the ring closure product, 2,3,4-triphenyl-1-naphthyllitium." See Ferman, J.; Kakareka, J.; Klooster, W. T.; Mullin, J. L.; Quatrucci, J. R.; Ricci, J.; Tracy, H. J.; Vining, W. J.; Wallace, S. *Inorg. Chem.* **1999**, *38*, 2464−2472.

(14) Gilman, H.; Cottis, S. G.; Atwell, W. H. *J. Am. Chem. Soc.* **1964**, *86*, 1596−1599.

(15) Corriu, R. J.-P.; Douglas, W. E.; Yang, Z.-X. *J. Organomet. Chem.* **1993**, *456*, 35−39.

(16) Tolan could be eluted much faster than the siloles using hexane/chloroform or chloroform/acetone mixture as eluent.

Table 1. Summary of Crystal Data and Intensity Collection Parameters for Siloles 3, 15, and 18

	3	15	18
empirical formula	$C_{40}H_{30}Si$	$C_{36}H_{26}Si$	$C_{44}H_{30}Si$
mol wt	538.73	486.66	586.77
crystal dimensions, mm	0.4 × 0.2 × 0.1	0.35 × 0.30 × 0.15	0.5 × 0.4 × 0.15
crystal system	triclinic	monoclinic	monoclinic
space group	$P\bar{1}$	$P2_1/c$	$P2_1/c$
unit cell constants			
a, Å	9.527(4)	18.5005(10)	10.792(2)
b, Å	10.043(4)	7.5768(4)	30.856(7)
c, Å	16.308(6)	21.7704(12)	11.130(3)
α, deg	77.150(7)	90	90
β, deg	79.580(7)	114.2430(10)	119.002(10)
γ, deg	71.981(7)	90	90
V, Å^3	1435.9(9)	2782.5(3)	3241.5(12)
Z	2	4	4
$D_{calcd.}$, g cm^{-3}	1.246	1.162	1.202
F_{000}	568	1024	1232
temp, K	100(2)	295(2)	100(2)
radiation (λ), Å	Mo Kα, 0.71070	Mo Kα, 0.71070	Mo Kα, 0.71070
μ(Mo Kα) mm^{-1}	0.110	0.106	0.103
$2\theta_{max}$, deg (completeness)	50 (85.0%)	50 (99.3%)	52 (99.5%)
no. of collected reflns	6141	25301	17359
no. of unique reflns. (R_{int})	4294 (0.0801)	4852 (0.0329)	6342 (0.0534)
data/restraints/parameters	4294/0/370	4852/0/335	6342/0/406
R_1, wR_2 [obs $I > 2\sigma(I)$]	0.0639, 0.1048	0.0554, 0.1303	0.0483, 0.1128
R_1, wR_2 (all data)	0.1002, 0.1150	0.0695, 0.1381	0.0660, 0.1185
goodness of fit, S	0.952	1.066	0.983
residual peak/hole e$^-$Å^{-3}	0.417/−0.297	0.313/−0.159	0.457/−0.349
transmission ratio	1.00/0.56	1.00/0.94	1.00/0.63

for tetraphenyl-substituted sila-, germana-, and stannacyclopentadienes, 23 hits, including a crystallographically isostructural tin analogue of **3**, $Ph_2Sn(CPh)_4$, were found.[13b] The silacyclopentadiene ring geometry in **3**, **15**, and **18** matched those of the 51 compounds in the CSD database. The average Si−C bond length over 160 observations from the database structures is 1.869(17) Å; in our siloles, the bond lengths Si1−C10 and Si1−C40 were all within 1 esd of this value (Table 2, nos. 1 and 2). The C=C and C−C distances around the central ring are 1.363(26) and 1.494(27) Å for 160 and 80 observations, respectively; in our siloles, these corresponding bond lengths were again all within a standard deviation of the average values.

The Si−C bonds of the substituents in **15** and **18** showed significant shortening for the *sp* hybridized ethynyl groups. The lengths of the exocyclic Si−C (*sp*) bonds in **15** [1.819(2) Å] and **18** [1.8231(18) and 1.8217(19) Å] are much shorter than those of the exocyclic Si−C (sp^2) bonds in **3** [1.874(3) and 1.864(3) Å] and **15** [1.852(2) Å] (Table 2, nos. 5 and 6). The Si−C (sp^2) bonds in **3** were somewhat stretched due to the steric effect of its two bulky phenyl groups, whereas in **15** this effect was lessened because it has only one phenyl group at the 1-position. Inspection of the ethynyl triple bonds revealed a shorter distance of 1.167(3) Å for C1−C2 in **15**, compared to 1.203 and 1.214(2) Å for the phenylethynyls in **18**. This is as expected because the triple bonds are lengthened through conjugation to the aromatic ring. The bond angles about the silole ring showed a typical pattern of a relatively small angle subtended at silicon itself C10−Si1−C40 93.2−94.6° (Table 2, no. 9), standard angles of 105.6−107.1° at C10 and C40 (nos. 10 and 11), and wider angles of between 116 and 117° at C20 and C30 (nos. 12 and 13).

All the three siloles contained a planar silacyclopentadiene ring, with torsion angles all less than |4.6|°

Table 2. Geometrical Parameters for the Crystal Structures of Siloles 3, 15, and 18

no.		3	15	18
		Bond Length (Å)		
1	endocyclic Si1−C10	1.874(3)	1.8655(19)	1.8719(17)
2	endocyclic Si1−C40	1.862(3)	1.854(2)	1.8668(19)
3	endocyclic C10−C20	1.357(4)	1.347(3)	1.365(3)
4	endocyclic C20−C30	1.501(4)	1.515(3)	1.517(2)
5	exocyclic Si−C	1.874(3)[a]	1.819(2)[b]	1.8231(18)[b]
6	exocyclic Si−C	1.864(3)[c]	1.852(2)[a]	1.8217(19)[d]
7	exocyclic C1−C2		1.167(3)	1.203(2)
8	exocyclic C3−C4			1.214(2)
		Bond Angle (deg)		
9	C10−Si1−C40	93.20(13)	93.82(9)	94.63(8)
10	Si1−C10−C20	106.3(2)	106.19(14)	105.61(13)
11	C30−C40−Si1	107.1(2)	106.87(14)	106.01(13)
12	C10−C20−C30	117.0(3)	116.80(17)	116.97(15)
13	C40−C30−C20	116.0(3)	116.10(18)	116.61(16)
14	Si1−C10−C11	124.2(2)	124.08(15)	123.92(13)
15	C10−C20−C21	124.6(3)	125.70(19)	127.30(16)
		Torsion Angle (deg)		
16	Si1−C10−C20−C30	−0.6(3)	4.6(2)	4.38(18)
17	C10−C20−C30−C40	−3.2(4)	−2.4(3)	−4.0
18	C16−C11−C10−C20	3.8(5)	−24.0(4)	−23.2
19	C46−C41−C40−C30	−39.5(5)	−26.0(3)	152.8(3)
20	C26−C21−C20−C30	−80.5(4)	−67.7(3)	87.6(2)
21	C32−C31−C30−C20	120.2(3)	−67.8(3)	109.2(2)

[a] Si1−C51. [b] Si1−C1. [c] Si1−C61. [d] Si1−C3.

(Table 2, nos. 16 and 17) and atomic displacements all less than 0.04 Å. As seen in the molecular plots of the siloles (cf. Figure 1), the tetraphenyl substituents at the ring carbons are twisted out of the plane of the silacyclopentadiene to varying extents, with typical dihedral angles to the phenyl planes of ~30° at the ring positions next to silicon (C10 and C40) and larger twists of ~70° at the C20 and C30 positions. The sense of the twist for all the four Ph substituents was typically the same, either all clockwise or all anticlockwise in a particular molecule. The centrosymmetric nature of the space groups for the siloles ensured that both "molecular hands" were found equally.

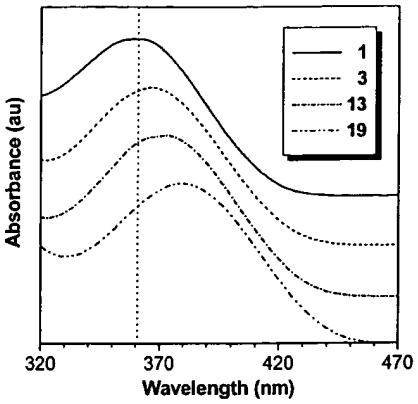

Figure 2. Electronic absorption spectra of chloroform solutions of siloles **1**, **3**, **13**, and **19**.

Electronic Transitions. We measured the absorption spectra of all the siloles, examples of which are given in Figure 2. The central silole ring of **1** absorbed in the UV region; when its 1,1-substituents were replaced by phenyls (**3**), the spectrum red-shifted. Bathochromic shift was also observed in the case of asymmetrically substituted 1,2,3,4,5-pentaphenylsiloles (**13** vs. **19**): introduction of a 1-hydroxyl group readily shifted the absorption spectrum to the red. Clearly, the silole rings are electronically perturbed by the 1,1-substituents.

The spectral characteristics of all the siloles are summarized in Table 3. The absorption spectrum of silole **1** peaked at 361 nm and the silole with one 1-methyl and one 1-phenyl (**2**) exhibited an absorption maximum (λ_{ab}) at 363 nm. Substituting a methyl of **2** by a phenyl (**3**) and changing from di- to monosubstitution (**13**) both red-shifted the λ_{ab} (Table 3, nos. 2–4); the extent of the bathochromic shift caused by the latter change was larger than that by the former, possibly due to the involved steric effect in the latter case. Comparison of the λ_{ab} values of **14**–**16** revealed that the absorption peaks of the siloles were insensitive to the change in the group attached to the other side (β position) of the triple bond (from methylenes to hydrogen to phenyl; Table 3, nos. 5–7). Similar results were observed for the pair of **17** and **18**: their λ_{ab} was not changed when the β-substituents changed from hydrogens to phenyls. These results suggest that the electronic structures of the siloles are influenced by the moieties directly attached to the central ring.

For the "symmetric" siloles with the same 1,1-substituents, their λ_{ab} was bathochromically shifted in the order of Me (**1**) < Ph (**3**) < C≡CR [R = H (**17**), Ph (**18**)]. For the disubstituted 1-phenylsiloles, the red-shift in λ_{ab} was in the order of Me (**2**) < Ph (**3**) < C≡CR (**14**–**16**) < OH (**19**). These sequences are in accordance with the increase in the electronegativity of the groups, which changes in the order of Me (2.3) < Ph (3.0) < C≡CH (3.3) < OH (3.7).[17] The inductive effect on the λ_{ab} observed here for the 1,1-substituted 2,3,4,5-tetraphenylsiloles is similar to that reported by Yamaguchi et al., who found that the electronic properties of another group of siloles, viz., 2,5-bis(trimethylsilyl)-3,4-diphenylsiloles, were mainly affected by the inductive effects of their 1,1-substituents.[18]

The molar absorptivities (ϵ_{max}) of the siloles are also given in Table 3; however, these exhibited no regular trend, suggesting that the ϵ_{max} is not a single function of the electronegativity of the substituents. The band gaps (E_g) of the siloles were calculated from the edges of their absorption spectra, which showed a clear correlation with λ_{ab}: when λ_{ab} was increased, E_g was generally decreased. Among the siloles, **1** and **19** exhibited the highest (2.95 eV) and lowest (2.79 eV) E_g values, respectively.

Solid-State Photoluminescence. Compared to the solution PL spectra, the solid-state data are more useful because they offer valuable information on how the luminophors perform in the real situation of aggregate state. As most people in the area normally do, we in our previous work measured the solid-state PL spectra of a few siloles by fabricating the thin solid films on quartz plates using a vacuum vapor deposition technique.[6] This process requires expensive equipment, needs large amounts of samples, and is wasteful, laborious, and time-consuming.[19] Moreover, the technique becomes invalid if the emitting species are thermally unstable and/or their melting points are too high.

Thin-layer chromatography (TLC) is widely used in synthetic chemistry as a handy tool for monitoring propagations of chemical reactions. Combinations of TLC with modern spectrometric techniques have led to the development of convenient analysis systems for product identifications, examples of which include TLC–MS, TLC–FTIR, TLC–Raman, and TLC–fluorescence.[20] The TLC–fluorescence system is very sensitive; the detection limit can go to the low picogram region. We are interested in expanding the usefulness of the TLC–fluorescence technique and tried to use the TLC plates as solid substrates for the measurements of solid-state PL spectra. We coated thin layers of siloles onto the solid substrates under ambient conditions by simply putting the TLC plates into the developing chambers containing the silole solutions. Under normal solution concentrations, macroscopically uniform silole layers spreading over the whole TLC plates were readily obtained.

The solid-state PL spectra of the silole layers absorbed on the TLC plates were measured, examples of which are given in Figure 3. When excited at 407 nm, the blank TLC plate emitted no detectable light in the spectral region of 410–750 nm, but the plate developed with a silole solution (0.5 mg/mL) emitted a strong light at 496 nm. When the concentration of the silole solution was increased (4.0 mg/mL), more silole molecules were absorbed onto the TLC plate and stronger light was emitted from the thicker silole layer. From the comparison with the PL spectrum of the thin solid film of **3** on a quartz plate (fabricated by the high-vacuum vapor deposition process[6]), it is clear that the emission maximum (λ_{em}) of the silole on the TLC plate is essentially

(17) Boyd, R. J.; Boyd, S. L. *J. Am. Chem. Soc.* **1992**, *114*, 1652–1655 and references therein.

(18) Yamaguchi, S.; Jin, R. Z.; Tamao, K. *J. Organomet. Chem.* **1998**, *559*, 73–80.

(19) Ktaft, A.; Grimsdale, A. C.; Holmes, A. B. *Angew. Chem., Int. Ed.* **1998**, *37*, 402–428.

(20) For reviews, see (a) Sherma, J. *Rev. Anal. Chem.* **1995**, *14*, 75–142. (b) Somsen, G. W.; Morden, W.; Wilson, I. D. *J. Chromatogr. A* **1995**, *703*, 613–665.

Table 3. Absorption and Emission Characteristics of 1,1-Substituted 2,3,4,5-Tetraphenylsiloles XYSi(CPh)$_4$ at Room Temperature

	1,1-substituents in silole			absorption[a]			emission	
no.	X	Y		λ_{ab}[b] (nm)	ϵ_{max}[c]/10^3	E_g[d] (eV)	λ_{em}[e] (nm)	Φ_F (%)[f]
1	CH_3	CH_3	**1**	361	8.83	2.95	481 (482)	22 (0.11)
2	Ph	CH_3	**2**	363	8.13	2.92	491 (494)	22 (0.09)
3	Ph	Ph	**3**	366	8.14	2.89	495 (499)	22 (0.10)
4	Ph	H	**13**	372	8.55	2.86	498 (500)	20 (0.09)
5	Ph	POD[g]	**14**	372	8.44	2.84	500 (504)	17 (0.10)
6	Ph	C≡CH	**15**	375	8.78	2.83	502 (504)	17 (0.11)
7	Ph	C≡CPh	**16**	375	9.11	2.83	502 (504)	18 (0.11)
8	C≡CH	C≡CH	**17**	378	9.27	2.81	505 (508)	20 (0.11)
9	C≡CPh	C≡CPh	**18**	378	8.82	2.80	505 (506)	18 (0.10)
10	Ph	OH	**19**	379	7.93	2.79	507 (510)	6 (0.11)

[a] Measured in chloroform. [b] Absorption maximum. [c] Molar absorptivity (mol^{-1} L cm^{-1}). [d] Band gap estimated from the absorption edge. [e] Emission maximum for thin layer of silole absorbed on TLC plate; data for corresponding silole in water/acetone mixture (9:1 by volume) are given in the parentheses. [f] Quantum yield of emission for silole nanoaggregates in water/acetone mixture (9:1 by volume); data for corresponding dilute solution in acetone are given in the parentheses. [g] POD = 8-phenyl-1,7-octadiynyl.

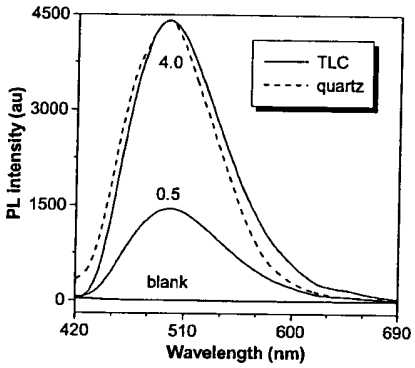

Figure 3. Solid-state photoluminescence spectra of thin layers of silole **3** absorbed on the TLC plates, which were developed with chloroform solutions of **3** (0.5 and 4.0 mg/mL). Excitation wavelength, 407 nm. Data for a blank TLC plate and a thin solid film of **3** on a quartz plate are shown for comparison.

identical to that on the quartz plate, proving the spectroscopic reliability of the simple TLC method.

The thin layers of other siloles absorbed on the TLC plates all fluoresced intensely; the λ_{em}'s are summarized in Table 3. Silole **1** emitted a blue light of 481 nm, and the emissions of other siloles were all red-shifted relative to that of **1**, with **19** emitting the reddest light (507 nm) among all the siloles. The trend of the red shift in the λ_{em} of the siloles generally mirrored that in their λ_{ab}, suggesting that the 1,1-substituents of the siloles exert a similar effect on their emission behaviors, or the inductive effect plays a major role in affecting their luminescence properties. Whereas the Stokes shift for silole **1** was 120 nm, all other siloles exhibited Stokes shifts of 127−129 nm.

Aggregation-Induced Emission. The TLC−PL experiments revealed that all the siloles were highly emissive in the solid state, and we further investigated whether the silole emissions, like that of **1**,[5] were also characterized with the AIE feature. In our previous study on the AIE phenomenon of **1**, we used ethanol as solvent,[5] and in this work we used acetone as solvent because of its strong solvating power in dissolving all the silole compounds. The dilute acetone solution of silole **3** (10 μM) was virtually nonemissive: even when its PL spectrum was magnified 100 times, only a noisy curve was obtained (Figure 4A). However, when a large amount (90%) of water, a poor solvent of **3**, was added

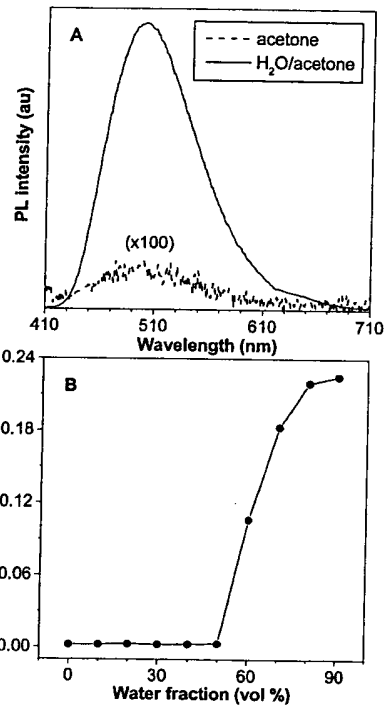

Figure 4. (A) Photoluminescence spectra of silole **3** in acetone and water/acetone mixture (9:1 by volume); concentration of **3**, 10 μM; excitation wavelength, 381 nm. (B) Quantum yield (Φ_F) of **3** vs composition of water/acetone mixture.

to the acetone solution (with the final concentration of the mixture being adjusted to 10 μM), an intense PL spectrum was recorded under identical measurement conditions. Clearly, **3** is AIE-active.

The huge difference in the PL intensity implies a big difference in the emission quantum yield (Φ_F). We estimated Φ_F of **3** in its acetone solution and water/acetone mixtures using 9,10-diphenylanthracene as standard.[21] The Φ_F of the acetone solution was as low as 0.0011 (Figure 4B). The Φ_F was almost unchanged when up to ~50 vol % water was added to the acetone solution but started to swiftly increase afterward. When the volume fraction of water in the water/acetone mixture was increased to 90%, Φ_F rose to 0.22, which

(21) Morris, J. V.; Mahaney, M. A.; Huber, J. R. *J. Phys. Chem.* **1976**, *80*, 969−974.

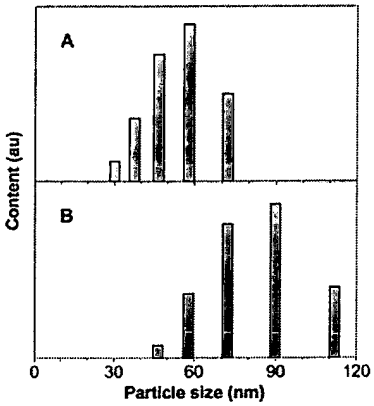

Figure 5. Size distributions of the nanoparticles of silole **3** in the water/acetone mixtures with (A) 70% and (B) 90% volume fractions of water; concentration of **3**, 10 μM.

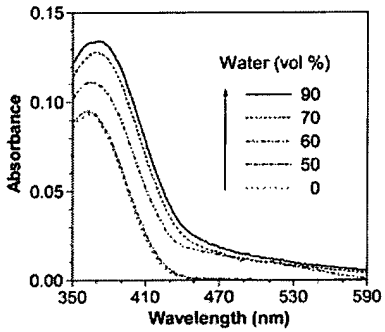

Figure 6. UV absorption spectra of silole **3** in water/acetone mixtures with different volume fractions of water; concentration of **3**, 10 μM.

was 200 times higher than that of the acetone solution. The trajectory of the Φ_F change suggests that the silole molecules started to aggregate at a water fraction of >50% and that the size and population of the aggregates continued to increase as the water fraction was increased.

Even at a water fraction as high as 90%, the water/acetone mixture of **3** was still visually clear and macroscopically homogeneous. The aggregates of the silole molecules thus must be of nanodimension. We measured the aggregate sizes and found that the silole particles in the water/acetone mixture with a 70% water fraction was in the range of ~30−72 nm, with an average particle size of ~53 nm (Figure 5). When the water fraction was increased to 90%, the sizes of the nanoparticles were increased to ~46−112 nm (with an average size of ~82 nm). However, when the water fraction was decreased to 60%, no reliable data could be obtained; the aggregates might be too small in size and too few in number to be detected by the particle size analyzer.

Figure 6 shows the absorption spectra of **3** in the water/acetone mixtures. The spectral profile was virtually unchanged when up to 50% water was added to the acetone solution. When the water fraction was further increased, the whole spectrum started to rise. The peak associated with the absorption of the silole ring slightly red-shifted: the λ_{ab} for the 90% mixture was 372 nm, whereas that for the acetone solution was 365 nm, the bathochromic shift being merely 7 nm. The increase in the absorbance in the whole spectral region was due to light scattering of the nanoaggregates,[22] which effectively decreased the light transmission through the silole mixtures. The abrupt increase in the absorbance from >50% water fraction agreed well with the sudden jump in the quantum yield shown in Figure 4B, double confirming that the silole molecules started to aggregate when >50% of the poor solvent (water) was added to the acetone solution.

Similar to **3**, other siloles were also essentially nonluminescent when molecularly dissolved in acetone at room temperature; their Φ_F values are tabulated in Table 3. The Φ_F of the siloles varied in a small range (0.09−0.11%), irrespective of the kinds of the 1,1-substituents. When the amounts of water added to the acetone solutions were enough to induce aggregate formation, all the siloles started to emit visible light; that is, the AIE is a general feature for all the silole emissions. The λ_{em} values for the water/acetone mixtures with 90% water fractions are also listed in Table 3. They correlated well with the data for the thin silole layers on the TLC plates, with discrepancies as small as 1−4 nm. The quantum yields of the light emission from the 90% water/acetone mixtures of all the siloles except for **19** were 17−22%, close to the Φ_F (21%) we previously reported for the emission of **2** from its water/ethanol mixture with a 90% water fraction.[5] The Φ_F of **19** was an outstanding exception and was as low as 6%, ~$^1/_3$ of those of the other siloles. The PL of the thin solid layer of **19** on the TLC plate was comparable to those of other siloles, suggesting that the much lower Φ_F of **19** in the water/acetone mixture is due to the amphiphilic nature of the silole molecule. Our attempts to measure the sizes of the nanoparticles of **19** in its water/acetone mixture with 90% water fraction failed: no detectable signals were recorded by the size analyzer, suggestive of much smaller and/or less clusters, if formed, in the solvent mixture. The relatively high polarity of the silole may have hampered its molecules from aggregating in the polar medium.

Restricted Intramolecular Rotation. The AIE effect is of technological value, considering that all-organic light-emitting materials are commonly used as thin solid films in their LED applications.[10,23] Aggregation normally quenches emission; what then is the real cause or mechanism for the "abnormal" AIE phenomenon?

Twisted intramolecular charge transfer (TICT) has been known to greatly affect emission properties of some chromophoric molecules containing donor and acceptor groups.[24,25] In such systems, polarity of solvent has been found to alter both ground and excited states of the

(22) (a) Sun, Q.; Xu, K.; Peng, H.; Zheng, R.; Häußler, M.; Tang, B. Z. *Macromolecules* **2003**, *36*, in press. (b) Sun, Q.; Lam, J. W. Y.; Xu, K.; Xu, H.; Cha, J. A. P.; Wong, P. C. L.; Wen, G.; Zhang, X.; Jing, X.; Wang, F.; Tang, B. Z. *Chem. Mater.* **2000**, *12*, 2617−2624. (c) Tang, B. Z.; Xu, H.; Lam, J. W. Y.; Lee, P. P. S.; Xu, K.; Sun, Q.; Cheuk, K. K. L. *Chem. Mater.* **2000**, *12*, 1446−1455. (d) Tang, B. Z.; Geng, Y.; Lam, J. W. Y.; Li, B.; Jing, X.; Wang, X.; Wang, F.; Pakhomov, A. B.; Zhang, X. X. *Chem. Mater.* **1999**, *11*, 1581−1589.

(23) (a) Kido, J.; Okamoto, Y. *Chem. Rev.* **2002**, *102*, 2357−2368. (b) Shim, H. K.; Jin, J. I. *Adv. Polym. Sci.* **2002**, *158*, 193−243. (c) Scherf, U.; List, E. J. W. *Adv. Mater.* **2002**, *14*, 477−487.

(24) (a) Rettig, W.; Baumann, W. In *Progress in Photochemistry and Photophysics*; Rabek, J. F., Ed.; CRC Press: Boca Raton, FL, 1990; Vol. 6, Chapter 3, pp 79−134. (b) Suppan, P. *Chemistry and Light*; Royal Society of Chemistry: London, 1994.

Table 4. Effect of Solvent Polarity on Absorption Maximums of Silole Solutions[a]

no.	solvent	$(\epsilon - 1)/(\epsilon + 2^b)$	λ_{ab} (nm) 3	18
1	cyclohexane	0.25	363	375
2	ethyl acetate	0.63	363	373
3	acetonitrile	0.92	360	370

[a] Concentration: 10 μM. [b] Debye solvent polarizability function.[26,27]

molecules. Increasing the polarity of solvents of 4-*N,N'*-dimethylaminoflavone solutions, for example, red-shifted their λ_{ab} and λ_{em} by up to >100 nm and enhanced their Φ_F by up to ~143 times.[26] The silole compounds are, however, not push–pull molecules. The solvent polarity, even when varied by ~3.7 times on the Debye scale, exerted little effect on their absorption transitions, as exemplified by the very small changes in the λ_{ab} of the silole solutions in different solvents (Table 4). Similarly, changing the solvent polarity hardly caused any changes in their emission transitions. We measured the PL spectra of the siloles in a variety of solvents with very different polarities (cyclohexane, toluene, dichloromethane, chloroform, carbon tetrachloride, ethyl acetate, THF, dioxane, acetone, acetonitrile, methanol, ethanol, etc.). All the solutions gave noisy spectra (cf., the PL spectrum of the acetone solution of **3** in Figure 4A); in other words, none of the solutions were luminescent, irrespective of the polarity of the solvents. These results evidently reduce the likelihood of the involvement of the TICT mechanism in the AIE processes of our silole system.

It is known that rotational energy relaxation can nonradiatively deactivate excited species.[28,29] In the solutions at room temperature, the active intramolecular rotations of the peripheral phenyl rings around the axes of the single bonds linked to the central silole ring may effectively annihilate the excitons, thus making the silole molecules nonemissive. In the solid aggregates, the stacking forces involved in the crystal packing may restrict the intramolecular rotations, which may block the nonradiative channel and populate the radiative decay, thus making the silole molecules luminescent. We envisioned that the siloles might become emissive even in their solutions by increasing the solution viscosity and/or by decreasing the solution temperature because both would hamper the intramolecular rotations. We thus examined the effects of viscosity and temperature on the emission behaviors of the silole molecules.

We first checked the viscosity effect on the silole emissions. Glycerol is a very viscous liquid, whose viscosity at 25 °C is 934 cp, ~1720 times higher than

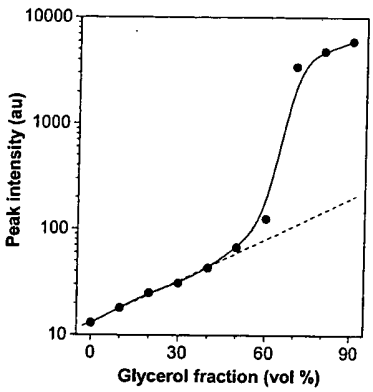

Figure 7. Photoluminescence peak intensity of silole **3** vs composition of glycerol/methanol mixtures; concentration of **3**, 10 μM; excitation wavelength, 407 nm.

that of methanol (0.544 cp).[30] Blending glycerol with methanol will thus afford liquid mixtures with drastically different viscosities. We measured the PL spectra of silole **3** in such mixtures and found that indeed the emission became stronger upon increasing the solution viscosity. The peak intensity of the PL spectrum "linearly" increased on the semilog scale when the glycerol fraction was increased from 0 to 50% (Figure 7), the PL intensity of the silole solution in the 50% glycerol/methanol mixture being ~5-fold higher than that in the methanol solution. The emission enhancement in this region should be predominantly due to the viscosity effect, because our previous work revealed that there were almost no aggregates even in the water/ethanol mixture with 50% water fraction (noting that water is an even poorer solvent of silole than glycerol).[5] The aggregation or AIE effect did come into play when the glycerol fraction was further increased, giving a plot similar to that shown in Figure 4B in the same region of poor solvent fractions (50–90%).

We then studied the temperature effect on the silole emissions. When a dilute dioxane solution of **18** (10 μM) was cooled, the intensity of its PL spectrum was increased (Figure 8A). The spectral profile hardly changed with temperature, suggesting that the emission is still associated with the radiative decay of the singlet excitons[7a] but not their triplet cousins. The peak intensity of the PL spectrum changed with temperature in a nonlinear fashion (Figure 8B). When cooled from room temperature to below the melting point of dioxane (11.8 °C), the liquid solution changed to a solid "glass". The intramolecular rotation may be restricted by the solid surroundings. The PL intensity was progressively increased when the temperature was successively decreased from 23 to −78 °C, indicating that the cooling is gradually limiting the thermally activated intramolecular rotations. Further decreasing the temperature from −78 °C to −196 °C caused little change in the peak intensity, implying that the intramolecular rotations may have already been frozen at −78 °C.

To separate the cooling effect from the "glass" effect or to see the "pure" temperature effect, we chose THF, a liquid with a high solvating power but a low melting point (−108 °C), which can keep the silole solute in the

(25) (a) Morozumi, T.; Anada, T.; Nakamura, H. *J. Phys. Chem. B* **2001**, *105*, 2923–2931. (b) Bajorek, A.; Paczkowski, J. *Macromolecules* **1998**, *31*, 86–95. (c) Soujanya, T.; Fessenden, R. W.; Samanta, A. *J. Phys. Chem.* **1996**, *100*, 3507–3512. (d) Grabowski, Z. R. *Pure Appl. Chem.* **1993**, *65*, 1751–1756.
(26) Wang, P.; Wu, S. *J. Luminescence* **1994**, *62*, 33–39.
(27) Debye, P. *Polar Molecules*; Dover: New York, 1945.
(28) (a) Malkin, J. *Photophysical and Photochemical Properties of Aromatic Compounds*; CRC Press: Boca Raton, FL, 1992. (b) *Photonic Polymer Systems*; Wise, D. L., Wnek, G. E., Trantolo, D. J., Cooper, T. M., Gresser, J. D., Eds.; Marcel Dekker: New York, 1998.
(29) (a) Wong, K. S.; Wang, H.; Lanzani, G. *Chem. Phys. Lett.* **1998**, *288*, 59–64. (b) Wong, K. S. personal communication.
(30) *CRC Handbook of Chemistry and Physics*, 75th ed.; Lide, D. R., Ed.; CRC Press: Boca Raton, FL, 1994; pp 6-241–6-245.

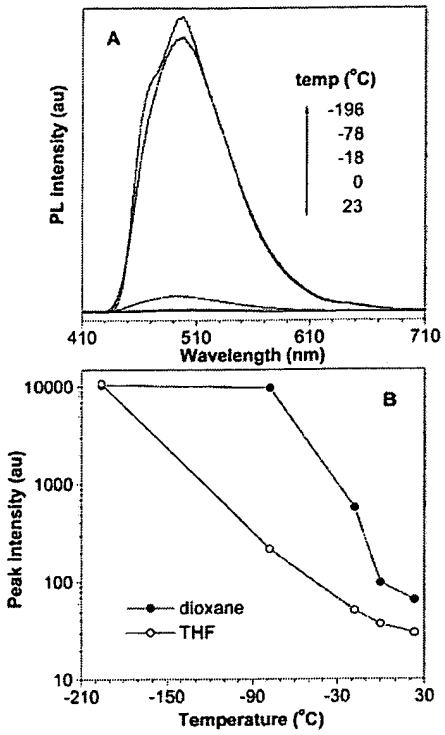

Figure 8. (A) Photoluminescence spectra of silole **18** in 1,4-dioxane at different temperatures. (B) Effect of temperature on the peak intensity of the photoluminescence of **18** in dioxane and THF. Concentration of **18**, 10 μM; excitation wavelength, 407 nm.

solution state at much lower temperatures. The peak intensity of the PL spectrum of a dilute THF solution of **18** at room temperature was weaker than that of its dioxane solution counterpart, due to the stronger solvating power of THF. The PL intensity of the silole solution increased with decreasing temperature in a nearly linear semilog fashion. THF has a low viscosity (0.456 cp at 25 °C) with a low-temperature coefficient (~0.008 cp/K).[30] The enhancement of the PL intensity above the melting point of the solvent thus should not be due to the viscosity effect but predominantly caused by the temperature effect; the cooling has restricted the thermally susceptible intramolecular rotations. Cooling the THF solution to −196 °C brought the intensity to a level comparable to that of the dioxane solution. The PL intensity at −196 °C was ~360-fold higher than that at room temperature.

To experimentally verify the restricted intramolecular rotations at the low temperatures, we carried out dynamic NMR (DNMR) experiments. The DNMR band shape analysis has been utilized in the studies of rotation-induced conformational changes in many systems, for example, the intramolecular rotations of isopropyl, dimethyl, and trineopentyl groups around the axes of the single bonds linked to the central rings of thiazoline-2-thione, diazole, and benzene, respectively.[31] The fast conformational exchanges caused by the fast intramolecular rotations upon the single-bond axes at

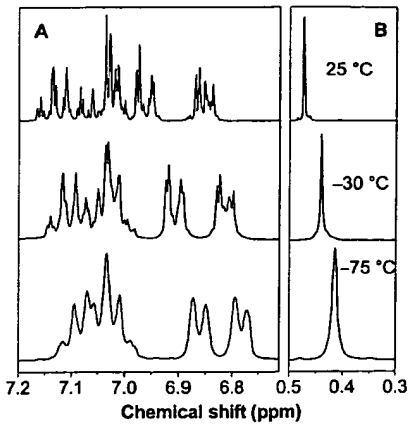

Figure 9. Resonance peaks of (A) phenyl and (B) methyl protons of silole **1** in dichloromethane-d_2 at different temperatures. The spectral peaks are not on the same vertical scales.

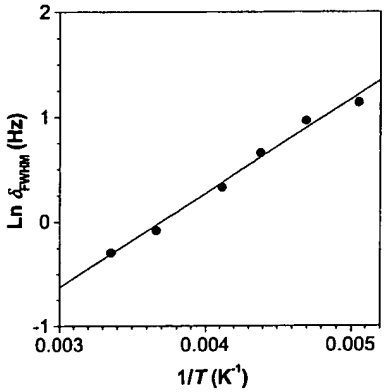

Figure 10. Effect of temperature (T) on the full width at half-maximum of the resonance peak (δ_{fwhm}) of methyl protons of silole **1**.

room temperature give sharp resonance peaks, whereas the slower exchanges due to the slowed rotations at lower temperatures broaden the resonance peaks.[31-33] The dichloromethane solution of silole **1** showed very sharp NMR peaks at room temperature, which clearly broadened when the temperature was decreased (Figure 9). The DNMR experiment thus confirms that the intramolecular rotations in the silole molecules have indeed been restricted at the low temperatures.

The band shape broadening in the downfield aromatic region resulted in the merger of neighboring resonance peaks of the 2,3,4,5-tetraphenyl protons, while that in the upfield aliphatic region was free of such complication, thus enabling us to quantify the temperature effect. The full width at half-maximum of the 1,1-dimethyl resonance peak (δ_{fwhm}) was successively increased when the solution temperature was gradually decreased (Figure 10). Dichloromethane has a low melting point (ca. −95 °C) and a low viscosity (~0.4 cp at 25 °C) with a low-temperature coefficient (~0.06 cp/K).[30] In the whole temperature range (25 to −75 °C), the solvent should be in the liquid state and experience little viscosity change. The solvating power of the

(31) (a) Lemaster, C. B. *Prog. Nucl. Magn. Reson. Spectr.* **1997**, *31*, 119−154. (b) Thornberry, M.; Slebodnick, C.; Deck, P. A.; Fronczek, F. R. *Organometallics* **2000**, *19*, 5352−5369. (c) Biedermann, P. U.; Stezowski, J. J.; Agranat, I. *Eur. J. Org. Chem.* **2001**, 15−34.

(32) (a) Carter, R. E.; Nilsson, B.; Olsson, K. *J. Am. Chem. Soc.* **1975**, *97*, 6155−6159. (b) Mislow, K. *Acc. Chem. Res.* **1976**, *9*, 26−33.

(33) (a) Sandström, J. *Dynamic NMR Spectroscopy*, Academic Press: London, UK, 1982. (b) Bovey, F. A.; Mirau, P. A. *NMR of Polymers*; Academic Press: San Diego, CA, 1996.

solvent should maintain unchanged, the silole molecules should remain molecularly dissolved, and their conformations should have thus not been affected by aggregate formation and viscosity change. The plot of ln δ_{fwhm} vs $1/T$ shown in Figure 10 is a linear line, suggesting that the band shape broadening follows a single mechanism. When the likelihood of aggregation formation and viscosity change is ruled out, the cooling-imposed restriction on the intramolecular rotations would be the single, or at least the predominant, cause for the band shape broadening.[34]

Concluding Remarks

We prepared a series of 1,1-substituted 2,3,4,5-tetraphenylsiloles using modified Curtis' procedures. To measure their solid-state PL spectra, we developed a TLC-based technique for preparing solid silole samples. The siloles absorbed on the TLC plates gave spectral data comparable to the "authentic" ones obtained from the thin films on the quartz plates fabricated by the vapor deposition process. Our new TLC-based technique is simple, reliable, and applicable to even thermally unstable and difficult-to-melt organic and organometallic compounds.

We studied the photophysical properties of the siloles and our key results are summarized as follows.

All the siloles were essentially nonluminescent when molecularly dissolved at room temperature but became highly emissive when induced to aggregate into nanoclusters. This proves that AIE is not an isolated phenomenon for a specific silole but a general feature for the whole group of siloles.[35]

Increasing the electronegativity of the 1,1-substituents of the siloles bathochromically shifted their λ_{ab} and λ_{em} and decreased their E_g. Their Φ_F was, however, almost unaffected by the structural variation.

Adding poor solvents, increasing viscosity, and decreasing temperature all boosted the Φ_F of the silole solutions (by up to ~360 times) but caused little changes in their λ_{ab} and λ_{em}.

The solution thickening and cooling experiments suggest that the AIE phenomenon is caused by the restricted intramolecular rotation. The blockage of the nonradiative channel via the rotational energy relaxation processes may have effectively populated the radiative decay of the excitons, thus turning "on" the silole emissions.

It becomes clear that the siloles are a group of novel molecules that are highly luminescent in their aggregation state. This unique emission feature makes the siloles promising candidate materials for an array of high-tech applications. For example, the siloles should be ideally suited for LED applications. Indeed, we made an LED device[36] of silole **3** and found that it worked impressively well: it was readily turned on at a low voltage (~4 V), emitted intensely at a moderate bias (55 880 cd/m^2 at 16 V), and showed very high emission efficiencies [15 cd/A (CE), 10 lm/W (PE), and 7% (η_{EL})]. The siloles may also serve as "molecular light switches"[37] for biosensor applications. Through appropriate chemical modifications, water-soluble amphiphilic siloles can be synthesized, which may be radiationless in physiological fluids. When entered into the hydrophobic pockets of biopolymers such as proteins and DNA, the siloles may aggregate and luminesce. The on–off switch of the light emission between the aggregate and nonaggregate states may be utilized for probing the folding and unfolding (or denaturing) processes accompanying the conformational changes of the biopolymers.[38] Research along this line is currently in progress in our laboratories, in collaboration with our biochemistry colleagues.

Experimental Section

Materials. THF and 1,4-dioxane (Aldrich) were predried over 4-Å molecular sieves and distilled from sodium benzophenone ketyl immediately prior to use. Triethylamine (RdH) was dried and distilled over KOH. Tolan or diphenylacetylene (**4**), trichlorophenylsilane, silicon(IV) chloride, lithium wire, copper(I) iodide, dichlorobis(triphenylphosphine)palladium(II), iodobenzene, phenylacetylene, 1,7-octadiyne, *n*-butyllithium (2.5 M in hexane), and ethynylmagnesium bromide (0.5 M in THF) were all purchased from Aldrich and used as received without further purification. Siloles **1**–**3** were prepared according to published experimental procedures.[6]

Instrumentation. The ^{1}H and ^{13}C NMR spectra were measured on a Bruker ARX 300 or a Varian Mercury 300 spectrometer using tetramethylsilane (TMS; δ = 0 ppm) or dichloromethane (δ = 5.32 ppm) as internal standard. The DNMR spectra were recorded on the Bruker ARX 300 spectrometer at 300.1 MHz using dichloromethane-d_2 as solvent. The FTIR spectra were taken on a Perkin-Elmer 16 PC spectrometer. The mass spectra were recorded on a Finnigan TSQ 7000 triple quadrupole spectrometer operating in a chemical ionization (CI) mode using methane as carrier gas. The UV–vis absorption spectra were measured on a Milton Roy Spectronic 3000 Array spectrophotometer.

The X-ray diffraction intensity data were collected at 295 or 100 K on a Bruker-Nonius Smart Apex CCD diffractometer with graphite-monochromated Mo Kα radiation. Single crystals of silole **3** were grown from methanol, whereas those of **15** and **18** were grown from toluene/heptane mixtures. Processing of the intensity data was carried out using the SAINT and SADABS routines, and the structure solution and refinement were carried out by the SHELXTL suite of X-ray programs (Version 6.10).

The PL spectra of the silole solutions and the nanoaggregate mixtures were recorded on a SLM 8000C spectrofluorometer. The sample chamber of the spectrofluorometer was dehumidified with P_2O_5. The nanoaggregate mixtures were freshly prepared by adding poor solvents into the silole solutions with vigorous shaking. For example, a nanoparticle mixture of **3** was prepared by adding 8 mL of water into 2 mL of an acetone solution of **3** in a 10-mL volumetric flask. The concentrations of all the nanoaggregate mixtures were adjusted to 10 μM. The particle sizes of the silole nanoaggregates in the water/acetone

(34) (a) Alberty, R. A.; Silbey, R. J. *Physical Chemistry*; Wiley: New York, 1992. (b) Goodman, L.; Pophristic, V.; Weinhold, F. *Acc. Chem. Res.* **1999**, *32*, 983–993. (c) Wiberg, K. B. *Acc. Chem. Res.* **1999**, *32*, 922–929.

(35) The AIE effect is probably a general characteristic for all metalloles because germoles also exhibit similar photophysical behaviors. Law, C. C. W.; Chen, J.; Tang, B. Z. *Polym. Prepr.* **2003**, *44* (1), in press.

(36) Configuration of the EL device: ITO/CuPc/TPD/**3**/Alq_3/LiF/Al, where ITO = indium tin oxide, CuPc = copper phthalocyanine, TPD = *N*, *N*-diphenyl-*N*, *N*-bis(3-methylphenyl)-1,1′-diphenyl-4, 4′-diamine, and Alq_3 = tris(8-hydroxyquinolinato)aluminum. Chen, H.; Chen, J.; Lam, J. W. Y.; Kwok, H. S.; Tang, B. Z. unpublished results.

(37) (a) Che, C. M.; Zhang, J.-L.; Lin, L.-R. *Chem. Commun.* **2002**, 2556–2557. (b) Mason, W. T. *Fluorescent and Luminescent Probes for Biological Activity*; Academic Press: London, 1999.

(38) Tang, B. Z. *Heart Cut* Nov. 25, 2002; http://chemistry.org/heartcut.html.

mixtures were measured on a Beckman Coulter Delsa 440SX Zeta potential analyzer.

For measurements of the solid-state PL spectra, the aluminum TLC plates (Merck, Silica 60 F_{254}) were used. The plates were cleaned by blowing them with compressed air and were then put into bottles containing the silole solutions for development. Chloroform solutions of the siloles with concentration of 2 mg/mL were generally used as developing media. In the specimen chamber of the SLM 8000C spectrofluorometer, the TLC plates coated with the thin silole layers were excited at an angle of 45° and the emitted light was collected at 135°.

Synthesis. Siloles **13**–**19** were prepared by the reaction routes shown in Schemes 1 and 2 from (di)chlorosilole intermediates **6** and **7**. The detailed experimental procedures for the synthesis of these siloles are given below.

1-Chloro-1,2,3,4,5-pentaphenylsilole (6). This intermediate was prepared according to a procedure reported by Curtis[12] with some modifications (see Results and Discussion section for details). Under dry nitrogen, 180 mg (25.9 mmol) of freshly cut lithium shavings was added to a solution of tolan **4** (6 g, 33.6 mmol) in 25 mL of THF. The mixture was stirred for 12 h at room temperature, and the resultant THF solution of **5** was added dropwise to a solution of trichlorophenylsilane (1.86 mL, 11.6 mmol) in 120 mL of THF. The mixture was refluxed for 5 h. The THF solution of the resultant reactive intermediate **6** was used in situ for the synthesis of siloles **13**–**16** and **19** without isolation.

1,1-Dichloro-2,3,4,5-tetraphenylsilole (7). The THF solution of **5**, prepared as described above, was added dropwise to a solution of silicon(IV) chloride (1.33 mL, 11.6 mmol) in 120 mL of THF. The mixture was stirred for 2 h at room temperature and then refluxed for 5 h. The THF solution of the resultant reactive intermediate **7** was used in situ for the synthesis of siloles **17** and **18**.

1-Phenyl-1,7-octadiyne (11). Into a 250-mL round-bottom flask were added copper(I) iodide (3 mg, 16 μmol), dichlorobis(triphenylphosphine)palladium(II) (0.42 g, 0.6 mmol), iodobenzene (3.43 mL, 30 mmol), and 1,7-octadiyne **10** (6.25 mL, 47 mmol) in 120 mL of triethylamine. The mixture was stirred at room temperature for 24 h. After filtration and solvent removal, the crude product was purified on a silica gel column using hexanes as eluent. Colorless oil of **11** was obtained in 68% yield (3.7 g). IR (KBr), ν (cm^{-1}): 3297 (≡C–H stretching), 637 (C≡C bending). ^1H NMR (300 MHz, $CDCl_3$), δ (TMS, ppm): 7.39 (m, 2H), 7.26 (m, 3H), 2.42 (m, 2H), 2.24 (m, 2H), 1.96 (s, 1H), 1.71 (m, 4H). ^{13}C NMR (75 MHz, $CDCl_3$), δ (TMS, ppm): 131.5, 128.1, 127.5, 123.9, 89.6, 84.1, 80.9, 68.5, 27.6, 27.5, 18.9, 17.9.

1,2,3,4,5-Pentaphenylsilole (13). Under vigorous stirring, the THF solution of **6** prepared as described above, was added dropwise to a suspension of $LiAlH_4$ (220 mg, 5.8 mmol) in 50 mL of THF at 0 °C. The mixture was allowed to warm to room temperature and was then stirred for 1 h. The excessive $LiAlH_4$ was quenched with 10 mL of ethyl acetate. The mixture was filtered and the crude product was purified on a silica gel column using hexane/chloroform mixture (3:1 by volume) as eluent. Product **13** (3.0 g) was isolated in 55% yield (based on trichlorophenylsilane used). Recrystallization from a toluene/heptane mixture gave 2.5 g of pure compound. Yellow-greenish solid: mp 190–192 °C. IR (KBr), ν (cm^{-1}): 2118 (Si–H stretching). ^1H NMR (300 MHz, $CDCl_3$), δ (TMS, ppm): 7.68 (d, 2H), 7.35 (m, 3H), 7.05–6.85 (m, br, 20H), 5.49 (s, 1H). ^{13}C NMR (75 MHz, $CDCl_3$), δ (TMS, ppm): 156.9, 138.7, 137.4, 135.6, 130.6, 130.3, 129.8, 129.3, 128.4, 127.9, 127.6, 126.5, 125.9. MS (CI): *m/e* 463 [$(M + 1)^+$]. UV ($CHCl_3$, 4.0×10^{-5} mol/L), λ_{max} (nm)/ϵ_{max} (mol^{-1} L cm^{-1}): $251/2.17 \times 10^4$, $372/8.55 \times 10^3$.

1-(8-Phenyl-1,7-octadiynyl)-1,2,3,4,5-pentaphenylsilole (14). Into a 100-mL round-bottom flask containing 10 mL of THF and 2.11 g (11.6 mmol) of 1-phenyl-1,7-octadiyne (**11**) was added dropwise 4.65 mL of a 2.5 M hexane solution of *n*-butyllithium (11.6 mmol) at ~0 °C under nitrogen. The mixture was stirred for 0.5 h, and the resultant 8-phenyl-1,7-octadiynyllithium **12** was added at room temperature into the THF solution of **6**. After stirring for 2 h, the mixture was filtered and the crude product was purified on a silica gel column using hexane/chloroform mixture (2:1 by volume) as eluent. Product **14** (4.2 g) was isolated in 57% yield (based on trichlorophenylsilane). Yellow-greenish solid: mp 62–64 °C. IR (KBr), ν (cm^{-1}): 2172 (C≡C stretching). ^1H NMR (300 MHz, $CDCl_3$), δ (TMS, ppm): 7.81 (d, 2H), 7.36 (m, 5H), 7.23 (m, 3H), 7.03–6.85 (m, 20H), 2.40 (m, 4H), 1.71 (m, 4H). ^{13}C NMR (75 MHz, $CDCl_3$), δ (TMS, ppm): 156.4, 138.7, 138.4, 137.4, 134.9, 131.5, 131.3, 130.2, 129.8, 129.3, 128.22, 128.15, 127.7, 127.53, 127.50, 126.47, 125.8, 123.9, 113.2, 89.7, 81.0, 77.0, 27.5, 27.3, 19.9, 18.9. MS (CI): *m/e* 643 [$(M + 1)^+$]. UV ($CHCl_3$, 4.0×10^{-5} mol/L), λ_{max} (nm)/ϵ_{max} (mol^{-1} L cm^{-1}): $253/4.05 \times 10^4$, $372/8.44 \times 10^3$.

1-Ethynyl-1,2,3,4,5-pentaphenylsilole (15). Into the THF solution of **6** was added dropwise 23.2 mL of a 0.5 M THF solution of ethynylmagnesium bromide (11.6 mmol) at room temperature. After stirring for 2 h, the mixture was filtered and the crude product was purified on a silica gel column using a mixture of hexane/chloroform (2:1 by volume) as eluent. Product **15** (1.8 g) was isolated in 32% yield (based on trichlorophenylsilane). Recrystallization from toluene/heptane mixture afforded 1.4 g pure compound. Yellow-greenish solid: mp 175–177 °C. IR (KBr), ν (cm^{-1}): 3252 (≡C–H stretching), 2035 (C≡C stretching). ^1H NMR (300 MHz, $CDCl_3$), δ (TMS, ppm): 7.78 (d, 2H), 7.37 (m, 3H), 7.03–6.85 (m, br, 20H), 2.70 (s, 1H). ^{13}C NMR (75 MHz, $CDCl_3$), δ (TMS, ppm): 157.1, 138.5, 138.0, 136.5, 135.0, 130.5, 130.0, 129.7, 129.2, 128.4, 127.8,127.6, 126.7, 126.0, 98.6, 82.5. MS (CI): *m/e* 487 [$(M + 1)^+$]. UV ($CHCl_3$, 4.0×10^{-5} mol/L), λ_{max} (nm)/ϵ_{max} (mol^{-1} L cm^{-1}): $249/2.36 \times 10^4$, $375/8.78 \times 10^3$.

1-(Phenylethynyl)-1,2,3,4,5-pentaphenylsilole (16). Into a 100-mL round-bottom flask containing 10 mL of THF and 1.27 mL of phenylacetylene (11.6 mmol) was added dropwise 4.65 mL of a 2.5 M hexane solution of *n*-butyllithium (11.6 mmol) at ~0 °C. The mixture was stirred for 0.5 h and the resultant THF solution of **9** was added dropwise into the THF solution of **6** at room temperature. After stirring for 2 h, the mixture was filtered and the crude product was purified on a silica gel column using hexane/chloroform mixture (2:1 by volume) as eluent. Product **16** (2.3 g) was isolated in 36% yield (based on trichlorophenylsilane used). Recrystallization from a toluene/heptane mixture gave 1.6 g pure compound. Yellow-greenish solid: mp 179–181 °C. IR (KBr), ν (cm^{-1}): 2156 (C≡C stretching). ^1H NMR (300 MHz, $CDCl_3$), δ (TMS, ppm): 7.87 (d, 2H), 7.54 (d, 2H), 7.33 (m, 6H), 7.04–6.88 (m, br, 20H). ^{13}C NMR (75 MHz, $CDCl_3$), δ (TMS, ppm): 156.7, 138.7, 138.3, 137.1, 135.0, 132.3, 130.9, 130.4, 129.8, 129.3, 129.2, 128.31, 128.27, 127.8, 127.6, 126.6, 125.9, 122.5, 110.3, 86.2. MS (CI): *m/e* 563 [$(M + 1)^+$]. UV ($CHCl_3$, 4.0×10^{-5} mol/L), λ_{max} (nm)/ϵ_{max} (mol^{-1} L cm^{-1}): $253/4.42 \times 10^4$, $375/9.11 \times 10^3$.

1,1-Diethynyl-2,3,4,5-tetraphenylsilole (17). Into the THF solution of **7**, prepared as described above, was added dropwise 46.4 mL of a 0.5 M THF solution of ethynylmagnesium bromide (23.2 mmol) at room temperature. After stirring for 2 h, the mixture was filtered and the crude product was purified on a silica gel column using hexane/chloroform mixture (2:1 by volume) as eluent. Product **17** (1.5 g) was isolated in 30% yield [based on silicon(IV) chloride]. Recrystallization from toluene/heptane mixture gave 1.2 g pure compound. Yellow-greenish solid: mp 199–201 °C. IR (KBr), ν (cm^{-1}): 3252 (≡C–H stretching), 2038 (C≡C stretching). ^1H NMR (300 MHz, $CDCl_3$), δ (TMS, ppm): 7.20–7.01 (m, br, 16H), 6.81 (m, 4H), 2.60 (s, 2H). ^{13}C NMR, (75 MHz, $CDCl_3$), δ (TMS, ppm): 157.4, 138.0, 137.2, 133.5, 129.5, 129.4, 128.0, 127.7, 126.9, 126.5, 97.6, 81.5. MS (CI): *m/e* 435 [$(M + 1)^+$]. UV ($CHCl_3$, 4.0×10^{-5} mol/L), λ_{max} (nm)/ϵ_{max} (mol^{-1} L cm^{-1}): $247/2.35 \times 10^4$, $378/9.27 \times 10^3$.

1,1-Bis(phenylethynyl)-2,3,4,5-tetraphenylsilole (18). Into the THF solution of **7** was added dropwise the THF solution of phenylethynyllithium **9** at room temperature. After stirring for 2 h, the mixture was filtered and the crude product was purified on a silica gel column using hexane/chloroform mixture (2:1 by volume) as eluent. Product **18** (3.3 g) was isolated in 48% yield [based on silicon(IV) chloride]. Recrys-

tallization from toluene/heptane mixture gave 2.9 g pure compound. Yellow-greenish solid: mp 214−216 °C. IR (KBr), ν (cm^{-1}): 2156 (C≡C stretching). ^1H NMR (300 MHz, $CDCl_3$), δ (TMS, ppm): 7.49 (m, 4H), 7.27 (m, 10H), 7.11 (m, 6H), 7.02 (m, 6H), 6.85 (m, 4H). ^{13}C NMR (75 MHz, $CDCl_3$), δ (TMS, ppm): 156.3, 138.2, 137.7, 134.8, 132.2, 129.5, 129.4, 129.1, 128.0, 127.7, 127.4, 126.5, 126.1, 122.1, 108.5, 85.7. MS (CI): *m/e* 587 [(M + 1)$^+$]. UV ($CHCl_3$, 1.0 × 10^{-5} mol/L), λ_{max} (nm)/ϵ_{max} (mol^{-1} L cm^{-1}): 255/6.03 × 10^4, 378/8.82 × 10^3.

*1-Hydroxy-1,2,3,4,5-pentaphenylsilole (**19**).* The solvent of the THF solution of **6** was evaporated and 100 mL of dry dichloromethane was added to redissolve the reactive intermediate. After filtration, the filtrate was added to 100 mL of 0.3% NH_4OH aqueous solution under vigorous stirring. The organic layer was separated and the crude product was purified on a silica gel column using hexane/chloroform mixture (1:2 by volume) as eluent. Product **19** (3.3 g) was isolated in 60% yield (based on trichlorophenylsilane). Yellow-greenish solid: mp 92−94 °C. IR (KBr), ν (cm^{-1}): 942 (Si−O stretching). ^1H NMR (300 MHz, $CDCl_3$), δ (TMS, ppm): 7.31 (m, 3H), 7.09 (t, 2H), 6.95 (m, 12H), 6.78 (m, 4H), 6.63 (m, 4H). ^{13}C NMR (75 MHz, $CDCl_3$), δ (TMS, ppm): 156.5, 141.5, 139.9, 138.6, 136.4, 131.5, 130.2, 129.7, 129.5, 128.1, 127.6, 127.0, 126.1, 125.5. MS (CI): *m/e* 479 [(M + 1)$^+$]. UV ($CHCl_3$, 4.0 × 10^{-5} mol/L), λ_{max} (nm)/ϵ_{max} (mol^{-1} L cm^{-1}): 251/2.38 × 10^4, 380/7.93 × 10^3.

Acknowledgment. The work described in this paper was partially supported by the Research Grants Council of the Hong Kong Special Administrative Region, China, through Grants HKUST 6187/99P, 6121/01P, and 6085/02P. This project also benefited from the financial support of the University Grants Committee (Hong Kong) under an Area of Excellence (AoE) Scheme (Project AoE/P-10/01-1-A). We thank Professor K. S. Wong of the Department of Physics of our University for his helpful discussions.

Supporting Information Available: Crystal structures with atom labels, tables of crystal data, structure solution and refinement, atomic coordinates, bond lengths and angles, and anisotropic displacement parameters (24 pages) for siloles **3** (CCDC 195948), **15** (CCDC 195949), and **18** (CCDC 195950) (PDF). Crystallographic information in CIF form is also available. These materials are available free of charge via the Internet at http://pubs.acs.org.

CM021715Z